

## Distinguishing natural from anthropogenic sources of acid extractable organics in groundwater near oil sands tailings ponds

Jason M.E. Ahad, Hooshang Pakdel, Paul R. Gammon, Bernhard Mayer, Martine M. Savard, Kerry M Peru, and John V. Headley

*Environ. Sci. Technol.*, **Just Accepted Manuscript** • DOI: 10.1021/acs.est.9b06875 • Publication Date (Web): 29 Jan 2020

Downloaded from [pubs.acs.org](https://pubs.acs.org) on February 4, 2020

### Just Accepted

“Just Accepted” manuscripts have been peer-reviewed and accepted for publication. They are posted online prior to technical editing, formatting for publication and author proofing. The American Chemical Society provides “Just Accepted” as a service to the research community to expedite the dissemination of scientific material as soon as possible after acceptance. “Just Accepted” manuscripts appear in full in PDF format accompanied by an HTML abstract. “Just Accepted” manuscripts have been fully peer reviewed, but should not be considered the official version of record. They are citable by the Digital Object Identifier (DOI®). “Just Accepted” is an optional service offered to authors. Therefore, the “Just Accepted” Web site may not include all articles that will be published in the journal. After a manuscript is technically edited and formatted, it will be removed from the “Just Accepted” Web site and published as an ASAP article. Note that technical editing may introduce minor changes to the manuscript text and/or graphics which could affect content, and all legal disclaimers and ethical guidelines that apply to the journal pertain. ACS cannot be held responsible for errors or consequences arising from the use of information contained in these “Just Accepted” manuscripts.



## 21 **ABSTRACT**

22 Distinguishing between naphthenic acids (NAs) associated with oil sands process-affected  
23 water (OSPW) and those found naturally in groundwaters in contact with the bituminous  
24 McMurray Formation poses a considerable analytical challenge to environmental research in  
25 Canada's oil sands region. Previous work addressing this problem combined high-resolution  
26 Orbitrap mass spectrometry with carbon isotope values generated by online pyrolysis ( $\delta^{13}\text{C}_{\text{pyr}}$ ) to  
27 characterise and quantify the acid extractable organics (AEOs) fraction containing NAs in the  
28 subsurface near an oil sands tailings pond. Here, we build upon this work through further  
29 development and application of these techniques at two different study sites near two different  
30 tailings ponds, in conjunction with the use of an additional isotopic tool – sulfur isotope analysis  
31 ( $\delta^{34}\text{S}$ ) of AEOs. The combined use of both  $\delta^{13}\text{C}_{\text{pyr}}$  and  $\delta^{34}\text{S}$  allowed for discrimination of AEOs  
32 into the three end-members relevant to ascertaining the NA environmental footprint within the  
33 region: 1) OSPW; 2) McMurray Formation groundwater (i.e., naturally occurring bitumen), and;  
34 3) naturally occurring non-bitumen. A Bayesian isotopic mixing model was used to determine the  
35 relative proportions of these three sources in groundwater at both study sites. Although background  
36 levels of OSPW-derived AEOs were generally low, one sample containing 49-99% (95%  
37 credibility interval) OSPW-derived AEOs was detected within an inferred preferential flow-path,  
38 highlighting the potential for this technique to track tailings pond seepage.

39

## 40 **INTRODUCTION**

41 The fate of the large volumes of oil sands process-affected water (OSPW) stored in tailings  
42 ponds is a major environmental concern in northern Alberta's Athabasca oil sands region (AOSR).  
43 Of particular interest is the acid extractable organics (AEOs) fraction containing naphthenic acids

44 (NAs) – a complex suite of alkyl-substituted acyclic and cycloaliphatic carboxylic acids generally  
45 considered the most toxic component of OSPW.<sup>1, 2</sup> Found naturally in bitumen, NAs become  
46 concentrated in OSPW during the extraction process associated with surface mining in the AOSR.  
47 Seepage of NAs from tailings ponds into surface water and groundwater poses a potential risk to  
48 local and downstream ecosystems and has thus been the subject of a growing number of  
49 investigations.<sup>3-10</sup>

50 Due to the potential for high background levels of naturally occurring, bitumen-derived  
51 AEOs in groundwater throughout the AOSR,<sup>4, 6, 11, 12</sup> techniques that are able to discriminate  
52 between these and mining-related inputs are critical for the accurate assessment of the mining  
53 industry's environmental footprint. The polar fractions of samples such as OSPW that consist  
54 predominantly of petroleum-derived constituents, however, are exceptionally complex mixtures  
55 containing tens of thousands of compounds.<sup>13, 14</sup> Such a high level of complexity, as revealed by  
56 recent advances in high- and ultrahigh-resolution mass spectrometry (see Headley et al.<sup>15</sup> and  
57 references therein) and multidimensional comprehensive gas chromatography mass spectrometry  
58 (GC × GC-MS),<sup>16-20</sup> does not facilitate accurate and quantitative source apportionment. Utilising  
59 high-resolution mass spectrometry (HRMS) analysis of AEOs, Frank et al.<sup>6</sup> reported the potential  
60 to differentiate natural from OSPW sources through the application of O<sub>2</sub>:O<sub>4</sub> species class ratios,  
61 owing to higher ratios in OSPW versus natural background containing bitumen-derived organics.  
62 However, other studies have reported wide ranges in O<sub>2</sub>:O<sub>4</sub> ratios for different sample types in the  
63 AOSR, implying non-unique end-member signatures and thus a limited usefulness for this  
64 approach in source discrimination.<sup>12, 21, 22</sup>

65 Another complementary technique that has shown potential to differentiate AEO sources  
66 in the AOSR, and which circumvents much of the inherent complexity associated with high- and

67 ultrahigh-resolution MS analysis, is thermal conversion/elemental analysis – isotope ratio mass  
68 spectrometry (TC/EA-IRMS), a technique that targets carboxyl-group carbon.<sup>23</sup> In conjunction  
69 with HRMS and natural abundance radiocarbon measurements, the carbon isotope ratios generated  
70 by online pyrolysis ( $\delta^{13}\text{C}_{\text{pyr}}$ ) using TC/EA-IRMS<sup>23</sup> were used to distinguish between bitumen-  
71 derived and non-bitumen-derived plant and soil organic matter AEOs along a groundwater flow  
72 path from a major oil sands tailings pond to the Athabasca River.<sup>4</sup> A two end-member isotopic  
73 mass balance used to determine the relative contributions of AEO sources in monitoring well  
74 samples was justified at this site due to hydrogeological assumptions and oil sands industry mining  
75 reports indicating no significant background concentrations of naturally occurring bitumen-  
76 derived polar organics in the shallow groundwater.

77         The lack of significant carbon isotopic variability between AEOs in OSPW and non-  
78 mining-related bituminous McMurray Formation groundwater implied that discrimination  
79 between different bitumen-derived polar organics would not be possible using only  $\delta^{13}\text{C}_{\text{pyr}}$   
80 values.<sup>4, 23</sup> However, additional isotopic characterisation of AEOs carried out in conjunction with  
81  $\delta^{13}\text{C}_{\text{pyr}}$  analysis could potentially overcome the limitations of the single isotope approach. For  
82 instance, the determination of both  $\delta^{13}\text{C}$  and  $\delta^2\text{H}$  values of polycyclic aromatic hydrocarbons in  
83 the AOSR allowed for a significantly more robust delineation of sources than provided by  $\delta^{13}\text{C}$   
84 analysis alone.<sup>24, 25</sup> In the case of AEOs, one of the obvious choices for additional isotopic  
85 characterisation is sulfur, which comprises a significant component of species classes (e.g.,  $\text{O}_x\text{S}_x$ ,  
86  $\text{S}_x$ ,  $\text{N}_x\text{O}_x\text{S}_x$ , etc.) found in a wide range of environmental samples from the AOSR.<sup>4, 6, 26, 27</sup> The  
87 analysis of isotope ratios ( $\delta^{34}\text{S}$ ) of total sulfur in AEOs, whether alone or in combination with  
88 another isotope ratio, has thus far not been reported in the AOSR. Hydrogen isotope ratios ( $\delta^2\text{H}$ )  
89 of AEOs were not considered due to the potential for isotopic exchange with labile H exchange

90 during sample processing. However, as it is possible to correct for this<sup>28, 29</sup>, future investigations  
91 could take advantage of a third additional isotopic tool.

92 Here we utilise HRMS in conjunction with  $\delta^{13}\text{C}_{\text{pyr}}$ , natural abundance radiocarbon ( $\Delta^{14}\text{C}$ )  
93 and  $\delta^{34}\text{S}$  ratios to characterise and quantify sources of AEOs in shallow groundwater monitoring  
94 wells near two oil sands tailings ponds. The wells are situated down the hydraulic gradients from  
95 the tailings ponds and adjacent to wetlands hosting abundant organic matter. The sites are different  
96 from that where the first investigation utilising HRMS,  $\delta^{13}\text{C}_{\text{pyr}}$  and  $\Delta^{14}\text{C}$  analyses occurred.<sup>4</sup>  
97 Samples from nearby surface waters and groundwater from the bituminous McMurray Formation  
98 were also analysed to provide reference comparisons. Principal Components Analysis (PCA) was  
99 carried out to examine trends in AEO distributions and a Bayesian isotopic mixing model  
100 incorporating  $\delta^{13}\text{C}_{\text{pyr}}$  and  $\delta^{34}\text{S}$  data was used to quantitatively estimate the relative proportions of  
101 the main sources of AEOs in groundwater.

102

## 103 **MATERIALS AND METHODS**

104 **Site Description and Sample Collection.** The two sites chosen for this study are located in the  
105 Athabasca oil sands active surface mining region situated north of the city of Fort McMurray,  
106 Alberta, Canada. Each site is owned and operated by a separate company, and bitumen extraction  
107 has occurred at both sites for approximately twenty years. The mining operations and associated  
108 tailings ponds fall within the watershed of the Muskeg River, a minor tributary of the Athabasca  
109 River, which itself flows northward into the Peace-Athabasca Delta.

110 All water samples were collected using fluorinated-HDPE containers rinsed at least three  
111 times prior to collection. Groundwater was collected following the purging of at least two well

112 volumes using a stainless steel bladder pump and after stabilization of pH, temperature, and  
113 conductivity.

114 Industry-installed groundwater monitoring wells situated in an organic-rich muskeg near  
115 Tailings Pond 1 (TP1) were sampled in October 2014. At two wells (GW1-4-2014, GW1-8-2014)  
116 the Quaternary muskeg deposits sit directly atop the bituminous Cretaceous McMurray Formation,  
117 while in the other wells there is a thin layer (< 2 m) of Quaternary till between the muskeg deposits  
118 and the McMurray Formation. The till in this area is mostly comprised of bituminous McMurray  
119 Formation.<sup>30</sup>

120 Samples from industry-installed groundwater monitoring wells near Tailings Pond 2 (TP2)  
121 were collected during three different autumn (September/October) field campaigns: 2015, 2016  
122 and 2017. These wells differ from those near TP1 in that they are screened in quartz-rich (i.e.  
123 minerallic-inorganic) Quaternary river sediments that overlie bituminous McMurray Formation  
124 sandstone. In addition to these pre-existing industry-installed wells, groundwater samples were  
125 collected in drive-point piezometers (DP samples) installed by Natural Resources Canada in 2016  
126 and 2017 in an organic-rich muskeg down-hydraulic gradient from both TP2 and the industry  
127 monitoring wells, and up-hydraulic gradient from the nearby Muskeg River.

128 OSPW was collected from TP1 in October 2014 and from TP2 during each of the 2015-  
129 2017 sampling campaigns. Pipe effluent located in the dyke system at the base of TP2 (labelled  
130 'seep-pipe') was also collected during 2015-2017. Surface water from nearby wetlands and  
131 streams and along the main stems of the Muskeg and Athabasca Rivers were collected during each  
132 of the four sampling periods (2014-2017). Groundwater not impacted by mining activities was  
133 collected from the bituminous McMurray Formation (MFGW) in 2014 and 2015 from two  
134 different wells installed by the companies operating the mines near TP1 and TP2 to provide

135 representative samples of naturally occurring bitumen-derived AEOs. Naturally occurring non-  
136 bitumen-derived AEOs (referred to henceforward as “non-bitumen”) are represented by two  
137 Pleistocene groundwater samples collected in 2014 and 2015 and by three samples of the Muskeg  
138 River collected upstream of oil sands mining activities during 2015-2017. The names (including  
139 year of collection), sample type and hydrogeochemical parameters of all water samples reported  
140 in this study are provided in the Supporting Information (Table S1).

141  
142 **Extraction of acid extractable organics (AEOs).** AEOs were extracted following protocols  
143 similar to those described previously.<sup>4, 23, 31</sup> In brief, between 1 to 12 L of water was acidified to  
144 pH 4.5 and extracted using loose Strata-X-A solid phase extraction sorbent (Phenomenex,  
145 Torrance, CA, USA) within several weeks after arriving from the field. The sorbent was then  
146 filtered from the aqueous phase under vacuum using pre-combusted glass fibre filters (450 °C for  
147 4h) and subsequently eluted with 10% formic acid in methanol and pure methanol. The extracts  
148 containing total AEOs were then evaporated to dryness under ultrahigh purity N<sub>2</sub>, re-dissolved in  
149 methanol and stored at 4 °C until subsequent analyses. Concentrations of AEOs in process blanks  
150 carried out using 12 L of Milli-Q water were < 1% of the mass of total AEOs in samples and are  
151 thus considered insignificant.

152  
153 **High-resolution mass spectrometry.** AEOs in subsamples sent to Environment and Climate  
154 Change Canada (Saskatoon, SK, Canada) were qualitatively and quantitatively analysed using a  
155 dual pressure linear ion trap high-resolution mass spectrometer (LTQ Orbitrap Elite, Thermo-  
156 Fisher Scientific, Bremen, Germany). Analyses were carried out by 5 µL loop injection (flow  
157 injection analysis) using a Surveyor MS pump (Thermo-Fisher) and a mobile phase of 50:50

158 acetonitrile/water containing 0.1% NH<sub>4</sub>OH. The Orbitrap was equipped with an ESI interface  
159 operated in negative ion mode, and data were acquired in full scan mode from m/z 100 to 600 at a  
160 setting of 240,000 resolution. The majority of ions were singly charged, and the average mass  
161 resolving power ( $m/\Delta m_{50\%}$ ) was 242,000 at m/z 400. Mass accuracies of less than 1 ppm were  
162 obtained using a lock mass compound (n-butyl benzenesulfonamide) for scan-to-scan mass  
163 calibration correction. Concentrations of AEOs from samples collected in 2014-2016 (Table S1)  
164 were determined in water subsamples extracted using solid-phase extraction (SPE) cartridges  
165 (ENV+, 200 mg, Biotage, Charlotte, NC); concentrations of AEOs from 2017 were not measured.  
166 Concentrations of AEOs were determined using a five point external standard calibration of  
167 Athabasca oil sands OSPW-derived AEOs at known concentrations as described elsewhere.<sup>6, 32</sup>

168  
169 **Carboxyl-group targeted carbon isotope analysis.** Carbon isotope ratios of the CO<sub>2</sub> generated  
170 by the pyrolytic decarboxylation of AEOs ( $\delta^{13}\text{C}_{\text{pyr}}$ ) were determined by thermal  
171 conversion/elemental analysis – isotope ratio mass spectrometry (TC/EA-IRMS) at the Delta-Lab  
172 of the Geological Survey of Canada (Québec, QC, Canada) using a Delta Plus XL isotope ratio  
173 mass spectrometer (Thermo-Fisher) following a protocol adapted from Ahad et al.<sup>23</sup>. The initial  
174 applications of this technique separated AEOs into distinct mass fractions using preparative  
175 capillary gas chromatography.<sup>4, 23</sup> However, because no significant isotopic variability was  
176 observed between the different mass fractions,<sup>23</sup> here we report  $\delta^{13}\text{C}_{\text{pyr}}$  values for unfractionated  
177 AEOs as done in a previous examination of NAs from undeveloped shale gas and tight oil  
178 reservoirs.<sup>31</sup> Briefly, aliquots of AEOs dissolved in methanol were transferred by syringe into a 40  
179  $\mu\text{L}$  rigid silver capsule (IVA-Analysentechnik e.K., Düsseldorf, Germany), dried in an oven at 60  
180 °C for 30 min, and sealed with pliers prior to analysis by TC/EA-IRMS using a pyrolysis reactor

181 temperature of 750 °C. The  $\delta^{13}\text{C}_{\text{pyr}}$  values were analysed using  $\text{CO}_2$  calibrated against international  
182 carbonate standards ( $\text{CO}_2$  obtained from Oztech Trading Corp., Safford, AZ, USA). Based on  
183 replicate standard and sample analyses, the uncertainty for  $\delta^{13}\text{C}_{\text{pyr}}$  values was  $\pm 0.6\%$ .

184

185 **Radiocarbon analysis.** Twelve subsamples of AEOs collected during the 2016 field campaign  
186 were analysed for natural abundance  $^{14}\text{C}$ . Aliquots of AEOs dissolved in methanol were transferred  
187 by syringe into a 40  $\mu\text{L}$  rigid silver capsule (IVA-Analysentechnik e.K., Düsseldorf, Germany),  
188 dried in an oven at 60 °C for 30 min, and sealed with pliers. The samples were submitted to the  
189 André E. Lalonde Accelerator Mass Spectrometry Laboratory at the University of Ottawa (Ottawa,  
190 ON, Canada) for  $^{14}\text{C}$  analysis using their 3MV tandem accelerator mass spectrometer (High  
191 Voltage Engineering Europa B.V., Amersfoort, the Netherlands) following in-house protocols for  
192 direct combustion of organic material.<sup>33</sup> Radiocarbon measurements are normalized to  $\delta^{13}\text{C}$  values  
193 (not reported here as they contain machine-associated isotopic fractionation) and reported as  $\Delta^{14}\text{C}$   
194 according to international convention.<sup>34</sup> The instrumental error associated with  $\Delta^{14}\text{C}$  analyses was  
195 less than 4%.

196

197 **Sulfur isotope analysis.** For samples collected in 2014-2016, sulfur isotope ratios ( $\delta^{34}\text{S}$ ) of total  
198 sulfur in AEOs dissolved in methanol were determined at the Department of Geoscience,  
199 University of Calgary. The samples were pipetted into smooth-walled tin cups containing  
200 Chromosorb (MilliporeSigma Canada Co., Oakville, ON), dried in an oven at 50°C for 1 h to  
201 remove solvent and then crimped prior to EA-IRMS analysis using an Elementar Isotope CUBE  
202 EA interfaced to a Thermo-Fisher Delta V Plus IRMS. Samples packed in tin capsules were  
203 dropped by an autosampler onto a quartz tube combustion reactor maintained at 1020 °C and

204 thermal decomposition was facilitated by addition of O<sub>2</sub>. The produced gases were then swept by  
205 the helium carrier through a purge and trap system prior to admitting the purified SO<sub>2</sub> into the ion  
206 source of the mass analyzer. δ<sup>34</sup>S values were determined by comparing the respective sample  
207 peak areas to those of reference gases alternately admitted to the ion source. Samples from 2017,  
208 in addition to several replicates (to test inter-lab comparability) and other samples from 2014-2016  
209 not previously analyzed, were run following a similar method yet without the use of Chromosorb  
210 and using 40 μL rigid silver capsules instead of tin capsules. These samples were analyzed at the  
211 Ján Veizer Stable Isotope Laboratory (University of Ottawa) using a CUBE EA interfaced to a  
212 Thermo-Fisher Delta Plus XP IRMS following flash combustion at 1800 °C. Raw sulfur isotope  
213 ratios were converted to δ<sup>34</sup>S values normalized to the internationally accepted V-CDT (Vienna -  
214 Canyon Diablo Troilite) scale using various reference materials. Based on replicate standard and  
215 sample analyses, the uncertainty for δ<sup>34</sup>S values was ±0.8‰ and ±0.4‰ for the first and second  
216 batch of samples, respectively.

217

## 218 **RESULTS AND DISCUSSION**

219 **AEO concentrations.** As observed in our previous examination of mining-related AEOs in  
220 groundwater in the AOSR,<sup>4</sup> the concentrations of AEOs (Table S1) were highest in OSPW (72.9  
221 ±7.8 mg/L) and generally lowest in downstream Muskeg River (4.2 ±2.6 mg/L), Athabasca River  
222 (1.4 ±0.2 mg/L) and other surface water samples (2.6 ±1.1 mg/L). AEOs in groundwater  
223 monitoring wells and drive point piezometers fell in an intermediate range (12.4 ±11.9 mg/L), as  
224 did MFGW samples (15.3 ±8.2 mg/L). The concentration of AEOs in the non-bitumen background  
225 samples were low (4.8 ±2.4 mg/L) and fell in a similar range to other surface water samples  
226 reported here (Table S1).

227

228 **High-resolution MS.** Results from Orbitrap MS analyses presented as the relative abundances  
229 (%) of the dominant species classes comprising AEOs (Table S2) show the highest proportions of  
230 O<sub>2</sub> in samples of tailings pond OSPW (65.3 ±7.3%) and McMurray Formation groundwater (58.5  
231 ±2.3%), as found previously in environmental samples from the AOSR.<sup>4</sup> The percentage of O<sub>2</sub>-  
232 containing species in the three upstream Muskeg River samples was low (4.8 ±2.9%) and similar  
233 to that found in downstream Muskeg River (8.3 ±5.6%), Athabasca River (3.1 ±2.2%) and other  
234 surface water samples (5.3 ±1.5%). The percentage of O<sub>2</sub>-containing species in the two Pleistocene  
235 groundwater samples (23.4 and 28.5%) was higher than that of surface water samples but low  
236 compared to OSPW and McMurray Formation groundwater. The proportions of O<sub>2</sub>-containing  
237 species in groundwater monitoring well samples from both sites (21.5 ±14.7%) generally fell in  
238 an intermediate range between OSPW / MFGW and that of non-bitumen. As observed during our  
239 previous investigation into sources of AEOs in groundwater near tailings ponds,<sup>4</sup> AEOs in surface  
240 water samples contained larger percentages of highly oxygenated (O<sub>5</sub> to O<sub>10</sub>) and nitrogen-  
241 containing (N<sub>x</sub>, N<sub>x</sub>S<sub>x</sub>, N<sub>x</sub>O<sub>x</sub> and N<sub>x</sub>O<sub>x</sub>S<sub>x</sub>) species compared to OSPW and MFGW (Table S2).  
242 While for the 2014 and 2015 field campaigns the percentages of sulfur-containing species (N<sub>x</sub>S<sub>x</sub>,  
243 N<sub>x</sub>O<sub>x</sub>S<sub>x</sub>, O<sub>x</sub>S<sub>x</sub> and S<sub>x</sub>) were in general greater in OSPW, MFGW and groundwater samples  
244 compared to surface water samples, this trend was not observed in 2016 and 2017 (Table S2).

245

246 **Carboxyl-group targeted carbon isotopes.** The overall trends in δ<sup>13</sup>C<sub>pyr</sub> values were also similar  
247 to those reported for the first application of this technique in the AOSR.<sup>4</sup> That is, the highest δ<sup>13</sup>C<sub>pyr</sub>  
248 values were found in OSPW (-20.7 ±0.4‰), whereas surface water and groundwater samples  
249 located down-gradient from the tailings ponds were as much as 8-9‰ lower (Table S1). The δ<sup>13</sup>C<sub>pyr</sub>

250 values for naturally occurring bitumen-derived AEOs (i.e., MFGW;  $-22.0 \pm 0.6\text{‰}$ ) were slightly  
251 lower than that of OSPW, and the five samples representing the non-bitumen end-member (i.e.,  
252 upstream Muskeg River and Pleistocene groundwater) were substantially lower ( $-27.9 \pm 0.6\text{‰}$ ) and  
253 similar to those in other surface water samples (Table S1).

254

255 **Radiocarbon isotopes.** The  $\Delta^{14}\text{C}$  values of AEOs from the 2016 sampling campaign (Table S3  
256 and Figure S1) ranged from a low of  $-987\text{‰}$  in OSPW, indicating a predominantly fossil carbon  
257 origin (i.e.,  $^{14}\text{C}$ -free;  $\Delta^{14}\text{C} = -1000\text{‰}$ ), to a high of  $-6\text{‰}$  in the Athabasca River sample, pointing  
258 to a primarily modern carbon source.  $\Delta^{14}\text{C}$  values for AEOs in the main branch of the Muskeg  
259 River near the confluence with the Athabasca River ( $-84\text{‰}$ ) and in the upstream background  
260 muskeg sample ( $-27\text{‰}$ ) also indicated a chiefly modern carbon origin. Groundwater samples had  
261  $\Delta^{14}\text{C}$  values ranging from  $-583$  to  $-952\text{‰}$ , indicating a mix between fossil and modern carbon  
262 sources (Table S3 and Figure S1).

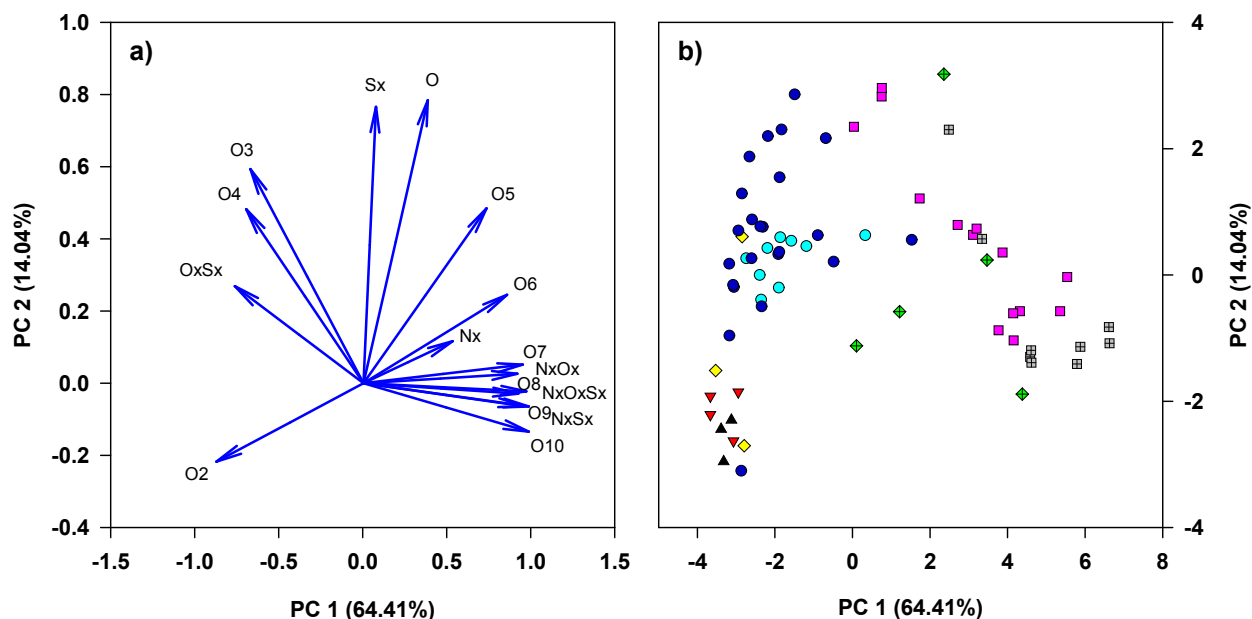
263

264 **Sulfur isotopes.** Sulfur isotope ratios ( $\delta^{34}\text{S}$ ) in AEOs ranged from  $0.3$  to  $10.2\text{‰}$  (Table S1), with  
265 the lowest values found in two samples from the main stem of the Athabasca River ( $0.3$  and  $1.8\text{‰}$ ),  
266 and the two highest values found in MFGW ( $8.8$  and  $10.2\text{‰}$ ). OSPW from four tailings ponds  
267 samples fell within a narrow range ( $6.8 \pm 0.4\text{‰}$ ), and the  $\delta^{34}\text{S}$  value determined for the non-bitumen  
268 samples was  $5.8 \pm 1.1\text{‰}$ . The values for monitoring well groundwater at both sites ( $6.7 \pm 0.9\text{‰}$ )  
269 fell between the values of OSPW/MFGW and that of the non-bitumen background. Sulfur isotope  
270 values for other surface water samples (not including the Athabasca River) ranged from  $3.0$  to  
271  $8.1\text{‰}$ .

272

273 **Qualitative evaluation of AEOs.** The distributions of species percentages ( $N_x$ ,  $N_xS_x$ ,  $N_xO_x$ ,  
274  $N_xO_xS_x$ ,  $O_xS_x$ ,  $O_1$  to  $O_{10}$  and  $S_x$ ) in AEOs were log-transformed ( $\log(x+1)$ ) and qualitatively  
275 examined via Principal Components Analysis (PCA) using SigmaPlot 14.0 (Systat Software Inc.,  
276 San Jose, CA). The PCA loadings (Figure 1a) and scores (Figure 1b) for the first (PC1) and second  
277 (PC2) principal components accounted for 65.26 and 14.04% of the total explained variance,  
278 respectively. PC1 was strongly ( $r > 0.5$ ) positively correlated with  $N_x$ ,  $N_xS_x$ ,  $N_xO_x$ ,  $N_xO_xS_x$  and  $O_5$   
279 to  $O_{10}$ , and strongly negatively correlated with  $O_xS_x$ ,  $O_2$ ,  $O_3$  and  $O_4$ . PC2 was strongly positively  
280 correlated with  $O$ ,  $O_3$  and  $S_x$ .

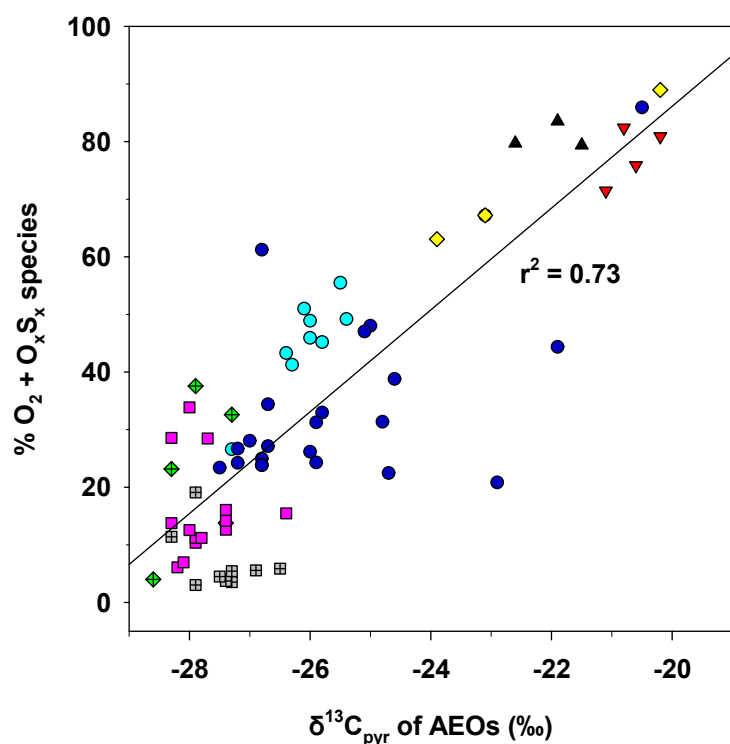
281 As illustrated on Figure 1b, the PCA scores plot revealed several distinct groupings for  
282 different sample types and sampling campaigns. Irrespective of collection date, the OSPW samples  
283 from both tailings ponds and MFGW samples were grouped together on the bottom left side of the  
284 plot and away from most of the other samples, chiefly as a function of their greater  $O_2$ -containing  
285 species component. Two of the three seep-pipe samples (2015 and 2017) also fell in this quadrant,  
286 with the seep-pipe sample from 2016 plotting slightly higher along the y-axis, in the region where  
287 the majority of groundwater samples from both study sites were located. The surface water samples  
288 generally plotted on the right side of Figure 1b and were grouped according to collection year,  
289 regardless of whether the sample originated from the Athabasca or Muskeg Rivers or a smaller  
290 stream. Samples from the 2017 field campaign grouped higher than the other years, and samples  
291 from 2014 and 2015 grouped together below those from 2016. Non-bitumen background AEOs  
292 were scattered near the surface water clusters and in a middle region between groundwater and  
293 surface water samples.



294  
295 **Figure 1.** Principal Components Analysis (PCA) loadings (a) and scores (b) carried out on log-transformed ( $\log(x+1)$ )  
296 species percentages of acid extractable organics (AEOs) in oil sands process-affected water (OSPW; inverted red  
297 triangles), McMurray Formation groundwater (MFGW; black triangles), monitoring well groundwater from Site 1  
298 (cyan circles) and Site 2 (dark blue circles), non-bitumen background (crossed green diamonds), Athabasca River  
299 (crossed gray squares), downstream Muskeg River and other surface waters (pink squares) and seep-pipe samples  
300 (yellow diamonds).

301  
302 Among the individual species classes shown on Figure 1, two appear to be potentially  
303 useful for tracking anthropogenic inputs in the AOSR:  $O_2$ , which includes classically-defined  
304 naphthenic (i.e., monocarboxylic) acids, and  $O_xS_x$ , which has been found in greater abundances in  
305 mining-related AEOs.<sup>4, 7, 27</sup> The relationship between  $\delta^{13}C_{pyr}$  values and the sum of  $O_2 + O_xS_x$   
306 species is shown on Figure 2 ( $r^2 = 0.73$ ,  $n = 70$ ,  $P < 0.0001$ ). In a manner similar to the trends  
307 found for PCA plots (Figure 1), the various sample types (i.e., non-bitumen background,  
308 Athabasca River, downstream Muskeg River and other surface waters, monitoring well  
309 groundwater from Sites 1 and 2, OSPW, MFGW and seep-pipe samples) plotted together in

310 distinct groupings. Samples with lower  $\delta^{13}\text{C}_{\text{pyr}}$  values (e.g., non-bitumen background, Athabasca  
311 River) were characterized by lower abundances of  $\text{O}_2 + \text{O}_x\text{S}_x$  species, whereas samples with higher  
312  $\delta^{13}\text{C}_{\text{pyr}}$  values (e.g., OSPW, MFGW) were generally associated with greater proportions of  $\text{O}_2 +$   
313  $\text{O}_x\text{S}_x$  (Figure 2). As illustrated on Figure 2, the majority of monitoring well groundwater samples  
314 from both sites fell between the non-bitumen background and OSPW / MFGW. Seep-pipe samples  
315 fell closer to OSPW / MFGW than to the non-bitumen end-member.



316  
317 **Figure 2.**  $\delta^{13}\text{C}_{\text{pyr}}$  versus the percentage of  $\text{O}_2 + \text{O}_x\text{S}_x$  species in acid extractable organics (AEOs) in oil sands process-  
318 affected water (OSPW; inverted red triangles), McMurray Formation groundwater (MFGW; black triangles),  
319 monitoring well groundwater from Site 1 (cyan circles) and Site 2 (dark blue circles), non-bitumen background  
320 (crossed green diamonds), Athabasca River (crossed gray squares), downstream Muskeg River and other surface  
321 waters (pink squares) and seep-pipe samples (yellow diamonds).

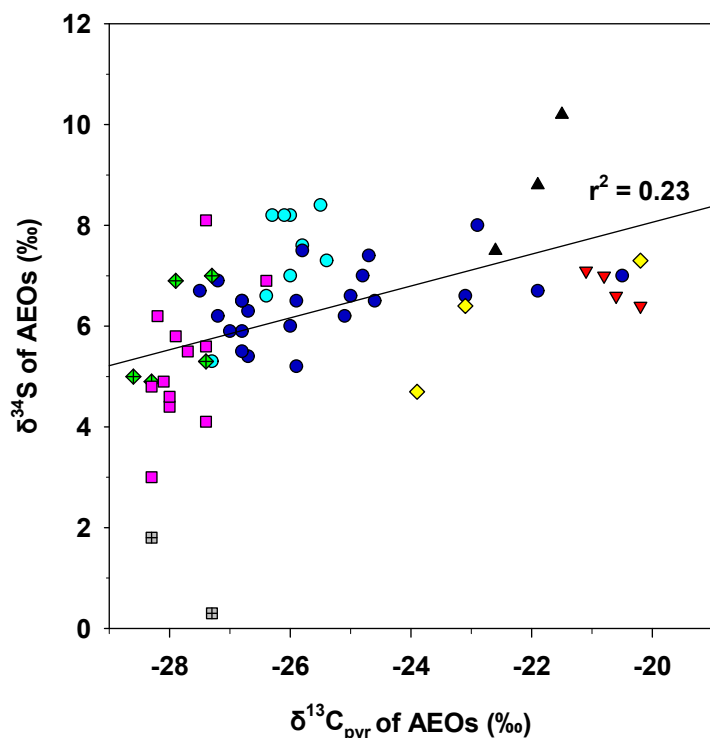
322

323 A similarly strong linear relationship between  $\delta^{13}\text{C}_{\text{pyr}}$  and  $\text{O}_2 + \text{O}_2\text{S}$  species for equivalent  
324 samples types (monitoring well groundwater, Athabasca River, OSPW and MFGW) was observed  
325 in the first application of  $\delta^{13}\text{C}_{\text{pyr}}$  analysis to characterise AEOs in the AOSR at a different tailings  
326 pond.<sup>4</sup> However, while this previous investigation was limited to only one sample of MFGW, here  
327 we report three MFGW samples from two different wells. A two-tailed Student's t-test indicated  
328 a significant difference ( $p < 0.05$ ) between  $\delta^{13}\text{C}_{\text{pyr}}$  values for OSPW ( $-20.7 \pm 0.4\text{‰}$ ) and MFGW ( $-$   
329  $22.2 \pm 0.6\text{‰}$ ), pointing to the possibility to distinguish between these two sample types. This  
330 suggests that the alkaline hot water extraction process used by commercial oil sands operations to  
331 extract bitumen may be associated with a small yet noticeable positive isotopic shift. As previously  
332 hypothesized but not corroborated by the sole MFGW sample available for comparison,<sup>23</sup> this shift  
333 may be the result of carboxyl group exchange with more  $^{13}\text{C}$ -enriched dissolved inorganic  
334 carbon.<sup>35</sup> Potential carboxyl-group exchange in AEOs deserves further investigation.

335 A much weaker linear relationship ( $r^2 = 0.23$ ,  $n = 61$ ,  $P < 0.0001$ ) was found between  
336  $\delta^{13}\text{C}_{\text{pyr}}$  and  $\delta^{34}\text{S}$  values (Figure 3). However, although  $\delta^{34}\text{S}$  values for non-bitumen background  
337 samples overlapped with those for OSPW, a subtle yet noticeable difference was observed between  
338  $\delta^{34}\text{S}$  values for OSPW and MFGW samples, which was confirmed by a Student's t-test ( $p < 0.05$ ).  
339 These samples were  $^{34}\text{S}$ -enriched compared to samples from the Athabasca River, one seep-pipe  
340 sample, and many of the downstream Muskeg River and other surface water samples (Figure 3).

341 Relatively low  $\delta^{34}\text{S}$  values found in highly degraded petroleum such as AOS bitumen have  
342 been attributed to the incorporation of  $^{34}\text{S}$ -depleted  $\text{H}_2\text{S}$  generated from bacterial sulfate reduction  
343 (BSR).<sup>36, 37</sup> Given that BSR is an important process in many tailings ponds,<sup>38, 39</sup> it is possible that  
344  $^{32}\text{S}$  becomes incorporated into OSPW-derived AEOs (including seep-pipe samples) during  
345 microbial reworking, thereby lowering its  $\delta^{34}\text{S}$  value in comparison to MFGW. However, since

346 BSR is also an important process within the bituminous McMurray Formation,<sup>40</sup> it is unclear why  
347 a slightly lower isotopic signal would be exhibited in OSPW and not MFGW samples. One  
348 possible explanation is that enhanced BSR in tailings ponds may be linked to microbial breakdown  
349 of constituents not present in great abundance in MFGW, such as the diluents (e.g., *n*-alkanes and  
350 BTEX) used to improve bitumen recovery rates.<sup>41</sup> Mixing with isotopically heavier Devonian  
351 fluids<sup>37</sup> in MFGW is another process that could lead to higher  $\delta^{34}\text{S}$  values in AEOs. This is  
352 supported by the high levels of total dissolved solids found in some MFGW samples across the  
353 AOSR, implying that on a local scale, highly saline formation waters in underlying Devonian strata  
354 can flow upwards into less saline or non-saline MFGW.<sup>42</sup> A better understanding of sulfur isotope  
355 dynamics in AEOs of bituminous samples is a goal of future research.



356  
357 **Figure 3.**  $\delta^{13}\text{C}_{\text{pyr}}$  versus  $\delta^{34}\text{S}$  values of acid extractable organics (AEOs) in oil sands process-affected water (OSPW;  
358 inverted red triangles), McMurray Formation groundwater (MFGW; black triangles), monitoring well groundwater

359 from Site 1 (cyan circles) and Site 2 (dark blue circles), non-bitumen background (crossed green diamonds), Athabasca  
360 River (crossed gray squares), downstream Muskeg River and other surface waters (pink squares) and seep-pipe  
361 samples (yellow diamonds).

362

363 The lower  $\delta^{34}\text{S}$  values found in non-bitumen background and surface water samples,  
364 particularly those for the Athabasca River (Figure 3), may also reflect incorporation of  $^{32}\text{S}$   
365 associated with BSR into the AEO pool. Similarly low  $\delta^{34}\text{S}$  values determined in dissolved organic  
366 matter in streams draining wetlands and forested catchments were attributed to incorporation of  
367 reduced inorganic sulfur into soil organic matter.<sup>43, 44</sup> The variation in  $\delta^{34}\text{S}$  of surface water and  
368 non-bitumen background AEOs found here may thus reflect variable proportions of BSR-derived  
369 soil organic matter.

370 The relationships between  $\Delta^{14}\text{C}$  and  $\text{O}_2 + \text{O}_x\text{S}_x$  species and between  $\Delta^{14}\text{C}$  and  $\delta^{13}\text{C}_{\text{pyr}}$  in  
371 AEOs for samples collected during the 2016 field campaign are presented in Figure S1. As  
372 observed in our previous study, the sample types with the largest percentages of  $\text{O}_2 + \text{O}_x\text{S}_x$  species  
373 and the highest  $\delta^{13}\text{C}_{\text{pyr}}$  values (i.e., OSPW and MFGW) had the lowest  $\Delta^{14}\text{C}$  values, pointing to a  
374 higher proportion of fossil carbon. Conversely, sample types with lower proportions of  $\text{O}_2 + \text{O}_x\text{S}_x$   
375 species and lower  $\delta^{13}\text{C}_{\text{pyr}}$  (i.e., Athabasca and Muskeg Rivers) contained higher  $\Delta^{14}\text{C}$  values,  
376 indicating a greater component of more recently fixed modern organic carbon.

377

378 **Quantitative source apportionment of AEOs in groundwater.** Collectively, the qualitative  
379 comparisons presented in Figures 1-3 and S1 demonstrate that monitoring well groundwater from  
380 Sites 1 and 2 contains a mixture of AEOs originating from the three main potential sources found  
381 in the shallow subsurface in the AOSR: non-bitumen background, OSPW and MFGW. However,  
382 accurate AEO source apportionment requires quantitative rather than qualitative analysis.

383 Advantageously, the large difference in  $\delta^{13}\text{C}_{\text{pyr}}$  between bitumen- and non-bitumen derived AEOs,  
384 combined with the small yet significant differences in  $\delta^{13}\text{C}_{\text{pyr}}$  and  $\delta^{34}\text{S}$  between OSPW and  
385 MFGW, point to the potential for an isotopic mixing model to provide quantification of mining-  
386 related NAs in groundwater samples from both study sites.

387         Employing a similar approach that used dual isotope ratios ( $\delta^{13}\text{C}$  and  $\delta^2\text{H}$ ) to quantify  
388 sources of phenanthrene deposited to a small lake in the Peace-Athabasca Delta,<sup>25</sup> here we applied  
389 a Bayesian isotopic mixing model (SIAR – Stable Isotope Analysis in R<sup>45</sup>) to quantify sources of  
390 AEOs in groundwater monitoring wells from Sites 1 and 2. A Bayesian-based mixing model using  
391  $\delta^{13}\text{C}_{\text{pyr}}$  and  $\delta^{34}\text{S}$  values was chosen over a simpler linear mixing model due to its ability to allow  
392 the propagation of the intrasource variability specific to each isotope ratio through the simulation.<sup>25</sup>  
393 Thus the uncertainties associated with the small isotopic differences between OSPW and MFGW  
394 are reflected in the model's output. As also performed by Jautzy et al.<sup>25</sup>, prior to running our data  
395 through SIAR, an initial assessment to determine whether the proposed source end-members can  
396 explain the isotope ratios of all groundwater monitoring well samples was made using another R-  
397 based model that simulates all possible mixing polygons by propagating the intrasource variability  
398 in a Monte Carlo simulation.<sup>46</sup>

399         For both the initial assessment of the mixing polygons and SIAR models, the following  
400 average  $\delta^{13}\text{C}_{\text{pyr}}$  and  $\delta^{34}\text{S}$  values for source end-members were used: non-bitumen background (-  
401  $27.9 \pm 0.6\text{‰}$ ;  $5.8 \pm 1.1\text{‰}$ ), OSPW ( $-20.7 \pm 0.6\text{‰}$ ;  $6.8 \pm 0.8\text{‰}$ ), and MFGW ( $-22.0 \pm 0.6\text{‰}$ ;  $8.8$   
402  $\pm 1.4\text{‰}$ ). In assigning error, the larger value between the intra-group variability and analytical  
403 uncertainty was applied ( $1\sigma$  standard deviation). The R-based models employed here were initially  
404 developed for understanding food-web dynamics; consequently, they require the input of a trophic  
405 enrichment factor (TEF) parameter to account for the isotopic offset between a predator and its

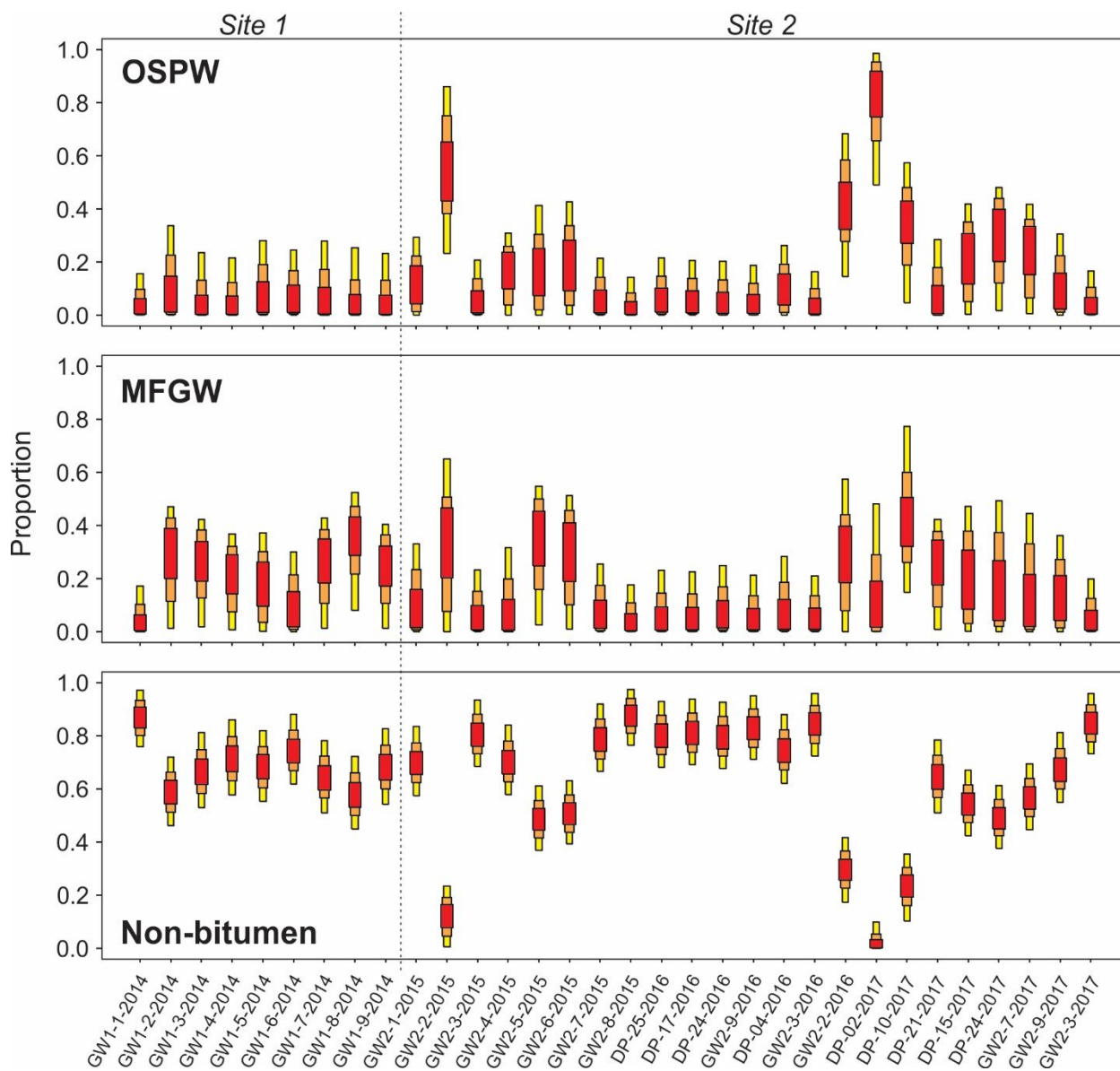
406 prey.<sup>46</sup> Since this parameter is not applicable to our dataset, TEF values were set to zero. The  
407 number of model iterations was set at 1500 for the mixing polygon assessment and 500,000 for  
408 the SIAR model.

409 As illustrated in Figure S2, groundwater samples fell predominantly within the area  
410 corresponding to the 95% mixing region, demonstrating that the selected source end-members are  
411 able to explain the isotopic variability at both sites. Proceeding with the SIAR model, the  
412 credibility intervals (CIs) for the proportion of each source in groundwater monitoring wells at  
413 Sites 1 and 2 were determined (Figure 4). As illustrated here, the majority of groundwater samples  
414 were comprised predominantly of non-bitumen- and MFGW-derived AEOs, with OSPW generally  
415 comprising a smaller component, particularly at Site 1 (0-34%; 95% CIs). An exception were four  
416 samples from Site 2 (GW2-2-2015, GW2-2-2016, DP-02-2017, DP-10-17), for which the upper  
417 95% CIs for OSPW ranged from 57-99% of AEOs. Wider 95% CIs were found for OSPW and  
418 MFGW compared to non-bitumen proportions, reflecting the smaller differences in isotope ratios  
419 between the two bitumen-derived AEO sources. Nonetheless, for the majority of groundwater  
420 monitoring wells, the ranges of estimated proportions for OSPW and MFGW were reasonably  
421 narrow; for instance, the differences between upper and lower 95% CIs were  $\leq 40\%$  in 19 out of  
422 32 wells for MFGW and 23 out of 32 wells for OSPW (Figure 4). The results of the SIAR model  
423 provided a quantitative estimate of OSPW in groundwater at two different mining operations, and  
424 revealed that at one of these sites (TP2), OSPW-derived NAs were the dominant source in several  
425 wells.

426 Two of the samples shown on Figure 4 that contained a high OSPW component were from  
427 the same well (GW2-2) sampled in 2015 (up to 86% OSPW; 95% CI) and 2016 (up to 68% OSPW;  
428 95% CI), indicating a persistent level of tailings pond seepage over time. Likewise, one well

429 sampled over the course of three years (GW2-3) revealed a consistently high proportion of non-  
430 bitumen background (68-96%; 95% CI) and low proportion of OSPW (0-21%; 95% CI). Higher  
431 maximum proportions of OSPW or MFGW in several wells (GW2-7, GW2-9, DP-24) in 2017 (up  
432 to 49%; 95% CI) compared to 2015-2016 (up to 25%; 95% CI) may have been the result of lower  
433 infiltration as 2017 was a drought year. Reduced precipitation leading to reduced infiltration likely  
434 results in smaller contributions of non-bitumen AEOs in the mixture and relatively greater  
435 fractions of bitumen-derived sources (i.e., Figure S1).

436



437

438

439 **Figure 4.** Proportion of AEOs derived from oil sands process-affected water (OSPW), McMurray Formation  
 440 groundwater (MFGW), and non-bitumen background determined using SIAR (Stable Isotope Analysis in R) in  
 441 monitoring well groundwater from Sites 1 and 2 (sites separated by the dotted vertical line). The red, orange, and  
 442 yellow boxes represent the 25, 75, and 95% credibility intervals (CIs), respectively.

443

444 To spatially visualize the results of the isotope mixing model, the mean proportions (with  
 445 95% CIs) of OSPW, MFGW and non-bitumen AEOs in monitoring wells along a groundwater

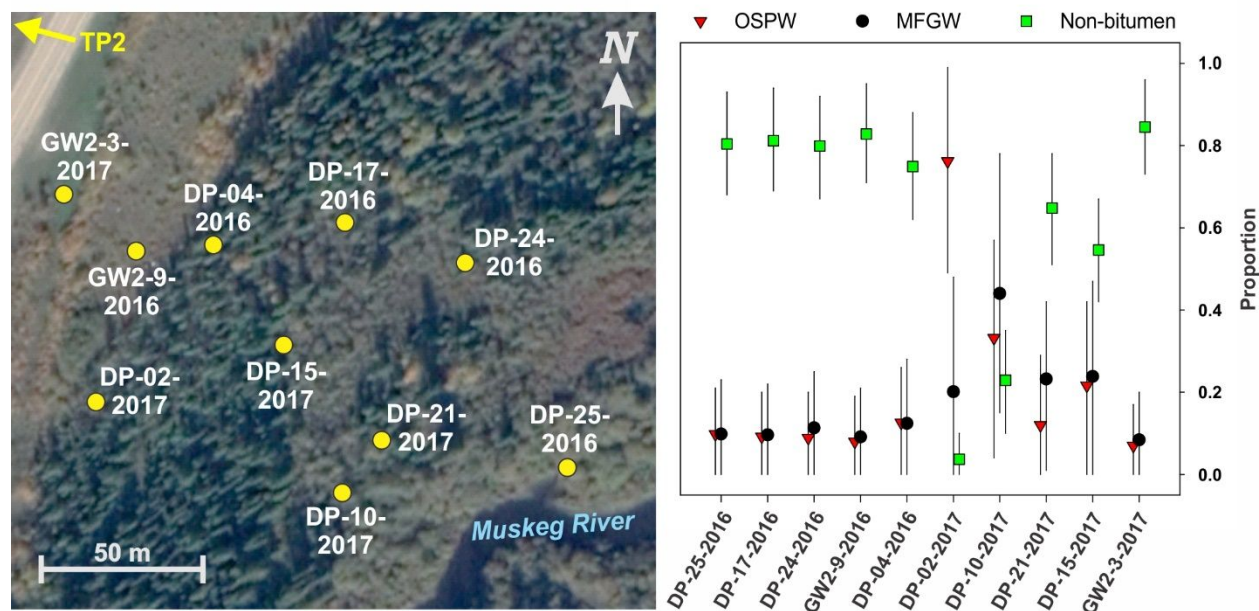
446 flow-path from the Site 2 tailings pond (TP2) to the Muskeg River in samples collected in either  
447 2016 or 2017 are shown together with their locations on Figure 5. As illustrated here, most of the  
448 wells contained relatively low proportions of OSPW (< 30% maximum; 95% CI), with the well  
449 located furthest down-gradient (DP-25-2016) indicating that significant levels of mining-related  
450 NAs were not reaching the Muskeg River. However, well DP-02-2017 had between 49-99%  
451 OSPW (95% CI), and a maximum of 57% OSPW (95% CI) was found in well DP-10-2017,  
452 indicating that tailings pond seepage may follow preferential flow-paths determined by localized  
453 variations in hydraulic conductivity.<sup>47</sup> The ability of the dual isotope approach to identify such  
454 occurrences in shallow groundwater systems adjacent to tailings ponds, and to distinguish OSPW  
455 from MFGW, provides a powerful tool for environmental monitoring in the AOSR. In conjunction  
456 with the information provided by high-resolution and other MS techniques, its application in  
457 further investigations is strongly encouraged.

458

459

460

461



462  
 463 **Figure 5.** Locations and mean proportions (error bars representing the 95% CIs) of OSPW, MFGW and non-bitumen  
 464 AEOs in monitoring wells along a groundwater flow-path from the Site 2 tailings pond (TP2; ~ 500 m off map in the  
 465 direction of the arrow) towards the Muskeg River; image obtained from Google Earth. The proportions of the three  
 466 main sources of AEOs were determined by the Bayesian isotopic mixing model (SIAR – Stable Isotope Analysis in  
 467 R) for samples collected in either 2016 or 2017.

468

## 469 ASSOCIATED CONTENT

### 470 Supporting Information

471 The Supporting Information is available free of charge at <https://pubs.acs.org/doi/...>

- 472 • Water sample information and hydrogeochemical parameters, percentages of dominant  
 473 species classes in AEOs determined by Orbitrap MS, radiocarbon data for twelve samples  
 474 of AEOs collected during 2016, relationships between  $\Delta^{14}\text{C}$  and  $\text{O}_2 + \text{O}_x\text{S}_x$  and between  
 475  $\Delta^{14}\text{C}$  and  $\delta^{13}\text{C}_{\text{pyr}}$  in AEOs, and the simulation of all possible mixing polygons incorporating  
 476 the average isotope ratios of AEOs for the three end-members (OSPW, MFGW and non-  
 477 bitumen).

478

479 **AUTHOR INFORMATION**480 **Corresponding Author**481 E-mail: [jason.ahad@canada.ca](mailto:jason.ahad@canada.ca)482 [orcid.org/0000-0003-3246-3950](https://orcid.org/0000-0003-3246-3950)

483 Phone: 1-418-654-3721

484

485 **ACKNOWLEDGMENTS**

486 The authors wish to thank staff at the GSC-Québec's Delta-lab (Jade Bergeron, Anna  
487 Smirnoff, Marc Luzincourt and Richard Huang), and Steve Taylor (University of Calgary) for help  
488 with sample preparation and laboratory analyses, Sam Morton and Stephanie Roussel for assisting  
489 with fieldwork, and Josué Jautzy for providing helpful comments that greatly improved the  
490 manuscript. We also wish to thank William Shotyk's team at the University of Alberta for  
491 providing Athabasca River samples in 2014. We are especially grateful to the several oil sands  
492 mining companies who facilitated this research with access to their monitoring wells and  
493 contextual data. This research was funded by Natural Resources Canada's Environmental  
494 Geoscience Program through the SOURCES Project. This is NRCan Contribution number  
495 20190306.

496

497 **REFERENCES**

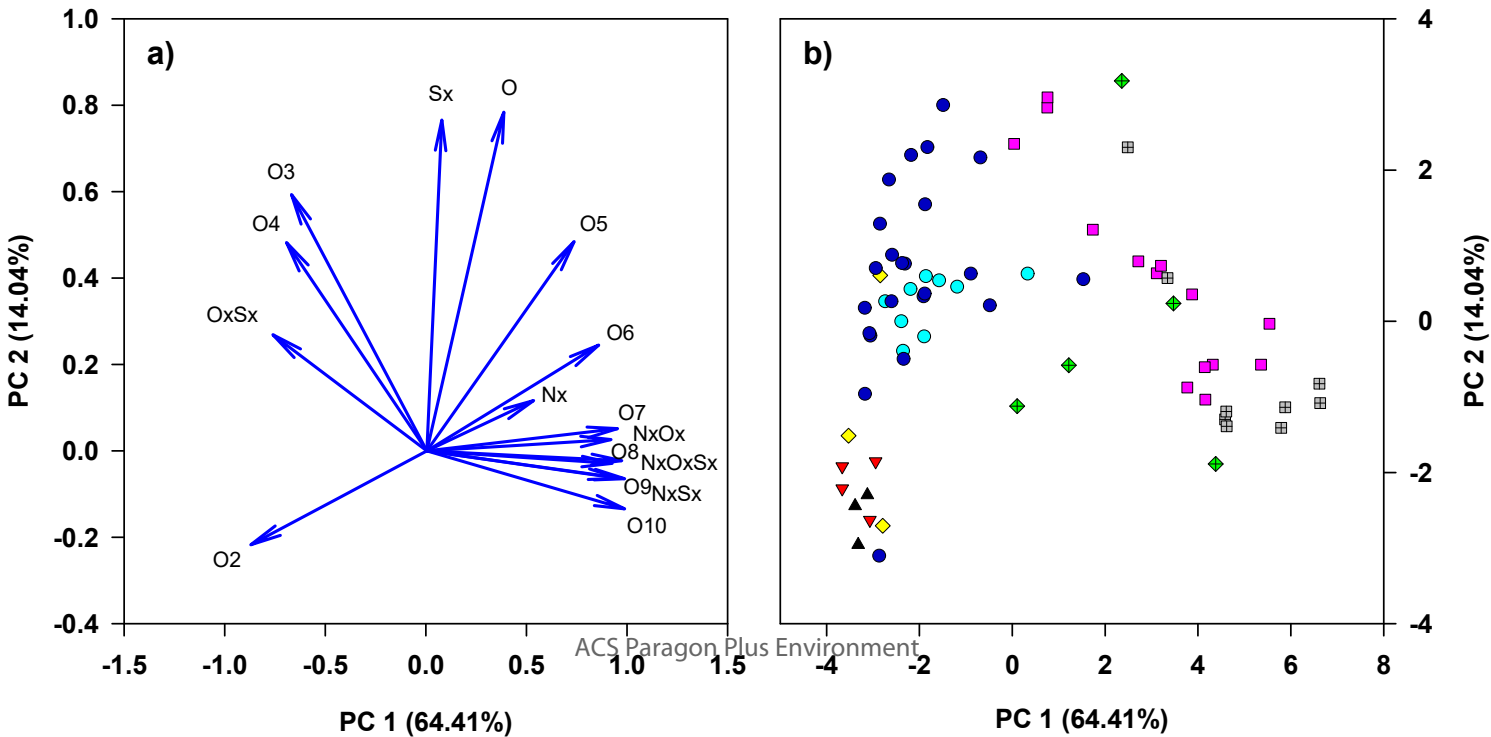
- 498 1. Li, C.; Fu, L.; Stafford, J.; Belosevic, M.; Gamal El-Din, M., The toxicity of oil sands process-affected  
499 water (OSPW): A critical review. *Sci. Total Environ.* **2017**, *601-602*, 1785-1802.
- 500 2. Morandi, G. D.; Wiseman, S. B.; Pereira, A.; Mankidy, R.; Gault, I. G. M.; Martin, J. W.; Giesy, J. P.,  
501 Effects-Directed Analysis of Dissolved Organic Compounds in Oil Sands Process-Affected Water. *Environ. Sci.*  
502 *Technol.* **2015**, *49*, (20), 12395-12404.

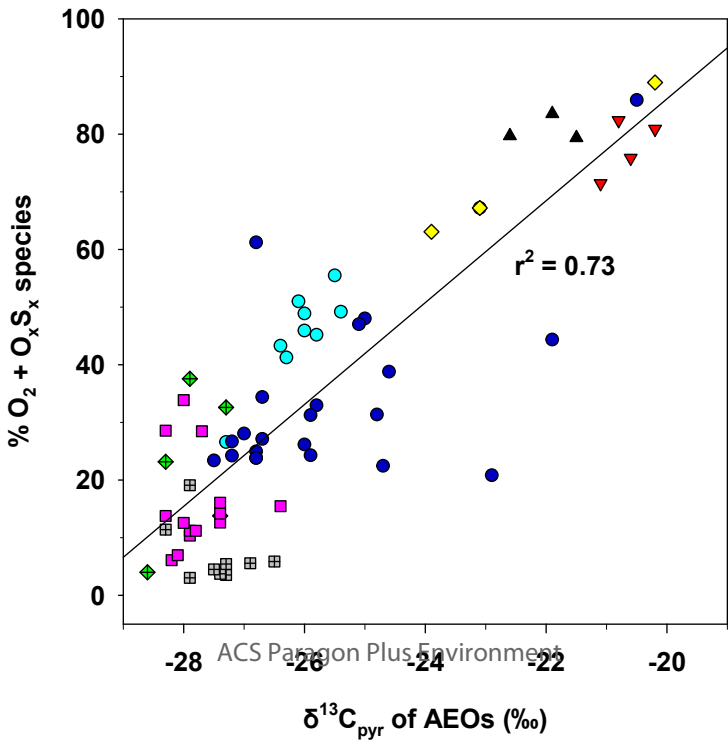
- 503 3. Ahad, J. M. E.; Pakdel, H.; Gammon, P. R.; Siddique, T.; Kuznetsova, A.; Savard, M. M., Evaluating in  
504 situ biodegradation of <sup>13</sup>C-labelled naphthenic acids in groundwater near oil sands tailings ponds. *Sci. Total*  
505 *Environ.* **2018**, *643*, 392-399.
- 506 4. Ahad, J. M. E.; Pakdel, H.; Savard, M. M.; Calderhead, A. I.; Gammon, P. R.; Rivera, A.; Headley, J. V.;  
507 Peru, K. M., Characterization and Quantification of Mining-Related “Naphthenic Acids” in Groundwater near a  
508 Major Oil Sands Tailings Pond. *Environmental Science & Technology* **2013**, *47*, (10), 5023–5030.
- 509 5. Fennell, J.; Arciszewski, T. J., Current knowledge of seepage from oil sands tailings ponds and its  
510 environmental influence in northeastern Alberta. *Sci. Total Environ.* **2019**, *686*, 968-985.
- 511 6. Frank, R. A.; Roy, J. W.; Bickerton, G.; Rowland, S. J.; Headley, J. V.; Scarlett, A. G.; West, C. E.; Peru,  
512 K. M.; Parrott, J. L.; Conly, F. M.; Hewitt, L. M., Profiling Oil Sands Mixtures from Industrial Developments and  
513 Natural Groundwaters for Source Identification. *Environmental Science & Technology* **2014**, *48*, (5), 2660–2670.
- 514 7. Huang, R.; Chen, Y.; Meshref, M. N. A.; Chelme-Ayala, P.; Dong, S.; Ibrahim, M. D.; Wang, C.;  
515 Klammerth, N.; Hughes, S. A.; Headley, J. V.; Peru, K. M.; Brown, C.; Mahaffey, A.; Gamal El-Din, M., Monitoring  
516 of classical, oxidized, and heteroatomic naphthenic acids species in oil sands process water and groundwater from  
517 the active oil sands operation area. *Sci. Total Environ.* **2018**, *645*, 277-285.
- 518 8. Oiffer, A. A. L.; Barker, J. F.; Gervais, F. M.; Mayer, K. U.; Ptacek, C. J.; Rudolph, D. L., A detailed field-  
519 based evaluation of naphthenic acid mobility in groundwater. *J. Contam. Hydrol.* **2009**, *108*, (3-4), 89-106.
- 520 9. Ross, M. S.; Pereira, A. d. S.; Fennell, J.; Davies, M.; Johnson, J.; Sliva, L.; Martin, J. W., Quantitative and  
521 Qualitative Analysis of Naphthenic Acids in Natural Waters Surrounding the Canadian Oil Sands Industry.  
522 *Environmental Science & Technology* **2012**, *46*, (23), 12796-12805.
- 523 10. Savard, M. M.; Ahad, J. M. E.; Gammon, P.; Calderhead, A. I.; Rivera, A.; Martel, R.; Klebek, M.;  
524 Headley, J. V.; Lefebvre, R.; Welsh, B.; Smirnoff, A.; Pakdel, H.; Benoit, N.; Liao, S.; Jautzy, J.; Gagnon, C.;  
525 Vaive, J.; Girard, I.; Peru, K. M. *A local test study distinguishes natural from anthropogenic groundwater*  
526 *contaminants near an Athabasca oil sands mining operation*; Geological Survey of Canada, Natural Resources  
527 Canada: Ottawa, 2012; p 140.
- 528 11. Kilgour, B.; Mahaffey, A.; Brown, C.; Hughes, S.; Hatry, C.; Hamilton, L., Variation in toxicity and  
529 ecological risks associated with some oil sands groundwaters. *Sci. Total Environ.* **2019**, *659*, 1224-1233.
- 530 12. Sun, C.; Shotyk, W.; Cuss, C. W.; Donner, M. W.; Fennell, J.; Javed, M.; Noernberg, T.; Poesch, M.;  
531 Pelletier, R.; Sinnatamby, N.; Siddique, T.; Martin, J. W., Characterization of Naphthenic Acids and Other  
532 Dissolved Organics in Natural Water from the Athabasca Oil Sands Region, Canada. *Environmental Science &*  
533 *Technology* **2017**, *51*, (17), 9524-9532.
- 534 13. McKenna, A. M.; Nelson, R. K.; Reddy, C. M.; Savory, J. J.; Kaiser, N. K.; Fitzsimmons, J. E.; Marshall,  
535 A. G.; Rodgers, R. P., Expansion of the Analytical Window for Oil Spill Characterization by Ultrahigh Resolution  
536 Mass Spectrometry: Beyond Gas Chromatography. *Environmental Science & Technology* **2013**, *47*, (13), 7530-  
537 7539.
- 538 14. Rowland, S. J.; Pereira, A. S.; Martin, J. W.; Scarlett, A. G.; West, C. E.; Lengger, S. K.; Wilde, M. J.;  
539 Pureveen, J.; Tegelaar, E. W.; Frank, R. A.; Hewitt, L. M., Mass spectral characterisation of a polar, esterified  
540 fraction of an organic extract of an oil sands process water. *Rapid Communications in Mass Spectrometry* **2014**, *28*,  
541 (21), 2352-2362.
- 542 15. Headley, J. V.; Peru, K. M.; Barrow, M. P., Advances in mass spectrometric characterization of naphthenic  
543 acids fraction compounds in oil sands environmental samples and crude oil—A review. *Mass Spectrometry Reviews*  
544 **2016**, *35*, (2), 311-328.

- 545 16. Rowland, S. J.; Scarlett, A. G.; Jones, D.; West, C. E.; Frank, R. A., Diamonds in the rough: Identification  
546 of individual naphthenic acids in oil sands process water. *Environ. Sci. Technol.* **2011**, *45*, (7), 3154-3159.
- 547 17. Rowland, S. J.; West, C. E.; Jones, D.; Scarlett, A. G.; Frank, R. A.; Hewitt, L. M., Steroidal aromatic  
548 Naphthenic Acids in oil sands process-affected water: Structural comparisons with environmental estrogens.  
549 *Environ. Sci. Technol.* **2011**, *45*, (22), 9806-9815.
- 550 18. Bowman, D. T.; Slater, G. F.; Warren, L. A.; McCarry, B. E., Identification of individual thiophene-,  
551 indane-, tetralin-, cyclohexane-, and adamantane-type carboxylic acids in composite tailings pore water from  
552 Alberta oil sands. *Rapid Communications in Mass Spectrometry* **2014**, *28*, (19), 2075-2083.
- 553 19. Bowman, D. T.; Jobst, K. J.; Ortiz, X.; Reiner, E. J.; Warren, L. A.; McCarry, B. E.; Slater, G. F., Improved  
554 coverage of naphthenic acid fraction compounds by comprehensive two-dimensional gas chromatography coupled  
555 with high resolution mass spectrometry. *Journal of Chromatography A* **2018**, *1536*, 88-95.
- 556 20. West, C. E.; Pureveen, J.; Scarlett, A. G.; Lengger, S. K.; Wilde, M. J.; Korndorffer, F.; Tegelaar, E. W.;  
557 Rowland, S. J., Can two-dimensional gas chromatography/mass spectrometric identification of bicyclic aromatic  
558 acids in petroleum fractions help to reveal further details of aromatic hydrocarbon biotransformation pathways?  
559 *Rapid Communications in Mass Spectrometry* **2014**, *28*, (9), 1023-1032.
- 560 21. Yi, Y.; Birks, S. J.; Cho, S.; Gibson, J. J., Characterization of organic composition in snow and surface  
561 waters in the Athabasca Oil Sands Region, using ultrahigh resolution Fourier transform mass spectrometry. *Sci.*  
562 *Total Environ.* **2015**, *518-519*, 148-158.
- 563 22. Yi, Y.; Gibson, J.; Birks, J.; Han, J.; Borchers, C. H., Comment on "Profiling Oil Sands Mixtures from  
564 Industrial Developments and Natural Groundwaters for Source Identification". *Environmental Science &*  
565 *Technology* **2014**, *48*, (18), 11013-11014.
- 566 23. Ahad, J. M. E.; Pakdel, H.; Savard, M. M.; Simard, M.-C.; Smirnoff, A., Extraction, separation and  
567 intramolecular carbon isotope characterization of Athabasca oil sands acids in environmental samples. *Anal. Chem.*  
568 **2012**, *84*, 10419-10425.
- 569 24. Jautzy, J.; Ahad, J. M. E.; Gobeil, C.; Savard, M. M., Century-long source apportionment of PAHs in  
570 Athabasca oil sands region lakes using diagnostic ratios and compound-specific carbon isotope signatures.  
571 *Environmental Science & Technology* **2013**, *47*, 6155-6163.
- 572 25. Jautzy, J. J.; Ahad, J. M. E.; Gobeil, C.; Smirnoff, A.; Barst, B. D.; Savard, M. M., Isotopic evidence for oil  
573 sands petroleum coke in the Peace-Athabasca Delta. *Environmental Science & Technology* **2015**, *49*, 12062-12070.
- 574 26. Headley, J. V.; Armstrong, S. A.; Peru, K. M.; Mikula, R. J.; Germida, J. J.; Mapolelo, M. M.; Rodgers, R.  
575 P.; Marshall, A. G., Ultrahigh-resolution mass spectrometry of simulated runoff from treated oil sands mature fine  
576 tailings. *Rapid Communications in Mass Spectrometry* **2010**, *24*, (16), 2400-2406.
- 577 27. Headley, J. V.; Barrow, M. P.; Peru, K. M.; Fahlman, B.; Frank, R. A.; Bickerton, G.; McMaster, M. E.;  
578 Parrott, J.; Hewitt, L. M., Preliminary fingerprinting of Athabasca oil sands polar organics in environmental samples  
579 using electrospray ionization Fourier transform ion cyclotron resonance mass spectrometry. *Rapid Communications*  
580 *in Mass Spectrometry* **2011**, *25*, (13), 1899-1909.
- 581 28. Ruppenthal, M.; Oelmann, Y.; Wilcke, W., Isotope ratios of nonexchangeable hydrogen in soils from  
582 different climate zones. *Geoderma* **2010**, *155*, (3), 231-241.
- 583 29. Wassenaar, L. I.; Hobson, K. A., Improved Method for Determining the Stable-Hydrogen Isotopic  
584 Composition ( $\delta D$ ) of Complex Organic Materials of Environmental Interest. *Environmental Science & Technology*  
585 **2000**, *34*, (11), 2354-2360.

- 586 30. Andriashek, L. D., *Quaternary geological setting of the Athabasca Oil Sands (in situ) area, northeast*  
587 *Alberta*. Alberta Energy and Utilities Board, Alberta Geological Survey: 2003.
- 588 31. Ahad, J. M. E.; Pakdel, H.; Lavoie, D.; Lefebvre, R.; Peru, K. M.; Headley, J. V., Naphthenic acids in  
589 groundwater overlying undeveloped shale gas and tight oil reservoirs. *Chemosphere* **2018**, *191*, (Supplement C),  
590 664-672.
- 591 32. Hughes, S. A.; Huang, R.; Mahaffey, A.; Chelme-Ayala, P.; Klammerth, N.; Meshref, M. N. A.; Ibrahim, M.  
592 D.; Brown, C.; Peru, K. M.; Headley, J. V.; Gamal El-Din, M., Comparison of methods for determination of total oil  
593 sands-derived naphthenic acids in water samples. *Chemosphere* **2017**, *187*, (Supplement C), 376-384.
- 594 33. Crann, C. A.; Murseli, S.; St-Jean, G.; Zhao, X.; Clark, I. D.; Kieser, W. E., First status report on  
595 radiocarbon sample preparation techniques at the AE Lalonde AMS Laboratory (Ottawa, Canada). *Radiocarbon*  
596 **2017**, *59*, (3), 695-704.
- 597 34. Stuiver, M.; Polach, H. A., Discussion: Reporting of  $^{14}\text{C}$  data. *Radiocarbon* **1977**, *19*, 355-363.
- 598 35. Dias, R. F.; Freeman, K. H.; Lewan, M. D.; Franks, S. G., delta C-13 of low-molecular-weight organic  
599 acids generated by the hydrous pyrolysis of oil-prone source rocks. *Geochim. Cosmochim. Acta* **2002**, *66*, (15),  
600 2755-2769.
- 601 36. Cai, C.; Worden, R. H.; Wolff, G. A.; Bottrell, S.; Wang, D.; Li, X., Origin of sulfur rich oils and H<sub>2</sub>S in  
602 Tertiary lacustrine sections of the Jinxian Sag, Bohai Bay Basin, China. *Appl. Geochem.* **2005**, *20*, (7), 1427-1444.
- 603 37. Méhay, S.; Adam, P.; Kowalewski, I.; Albrecht, P., Evaluating the sulfur isotopic composition of  
604 biodegraded petroleum: The case of the Western Canada Sedimentary Basin. *Org. Geochem.* **2009**, *40*, (4), 531-545.
- 605 38. Ramos-Padrón, E.; Bordenave, S.; Lin, S.; Bhaskar, I. M.; Dong, X.; Sensen, C. W.; Fournier, J.;  
606 Voordouw, G.; Gieg, L. M., Carbon and sulfur cycling by microbial communities in a gypsum-treated oil sands  
607 tailings pond. *Environmental science & technology* **2010**, *45*, (2), 439-446.
- 608 39. Stasik, S.; Loick, N.; Knöller, K.; Weisener, C.; Wendt-Potthoff, K., Understanding biogeochemical  
609 gradients of sulfur, iron and carbon in an oil sands tailings pond. *Chem. Geol.* **2014**, *382*, 44-53.
- 610 40. Birks, S. J.; Fennell, J. W.; Gibson, J. J.; Yi, Y.; Moncur, M. C.; Brewster, M., Using regional datasets of  
611 isotope geochemistry to resolve complex groundwater flow and formation connectivity in northeastern Alberta,  
612 Canada. *Appl. Geochem.* **2019**, *101*, 140-159.
- 613 41. Gee, K. F.; Poon, H. Y.; Hashisho, Z.; Ulrich, A. C., Effect of naphtha diluent on greenhouse gases and  
614 reduced sulfur compounds emissions from oil sands tailings. *Sci. Total Environ.* **2017**, *598*, 916-924.
- 615 42. Cowie, B. R.; James, B.; Mayer, B., Distribution of total dissolved solids in McMurray Formation water in  
616 the Athabasca oil sands region, Alberta, Canada: Implications for regional hydrogeology and resource  
617 development Distribution of Total Dissolved Solids in McMurray Formation Water. *AAPG Bulletin* **2015**, *99*, (1),  
618 77-90.
- 619 43. Giesler, R.; Björkvald, L.; Laudon, H.; Mörth, C.-M., Spatial and seasonal variations in stream water  $\delta^{34}\text{S}$ -  
620 dissolved organic matter in Northern Sweden. *Environmental science & technology* **2008**, *43*, (2), 447-452.
- 621 44. Kang, P.-G.; Mitchell, M. J.; Mayer, B.; Campbell, J. L., Isotopic evidence for determining the sources of  
622 dissolved organic sulfur in a forested catchment. *Environmental science & technology* **2014**, *48*, (19), 11259-11267.
- 623 45. Parnell, A. C.; Inger, R.; Bearhop, S.; Jackson, A. L., Source partitioning using stable isotopes: coping with  
624 too much variation. *PloS one* **2010**, *5*, (3), e9672.

- 625 46. Smith, J. A.; Mazumder, D.; Suthers, I. M.; Taylor, M. D., To fit or not to fit: evaluating stable isotope  
626 mixing models using simulated mixing polygons. *Methods in Ecology and Evolution* **2013**, *4*, (7), 612-618.
- 627 47. Ferguson, G.; Rudolph, D.; Barker, J., Hydrodynamics of a large oil sand tailings impoundment and related  
628 environmental implications. *Canadian Geotechnical Journal* **2009**, *46*, (12), 1446-1460.  
629





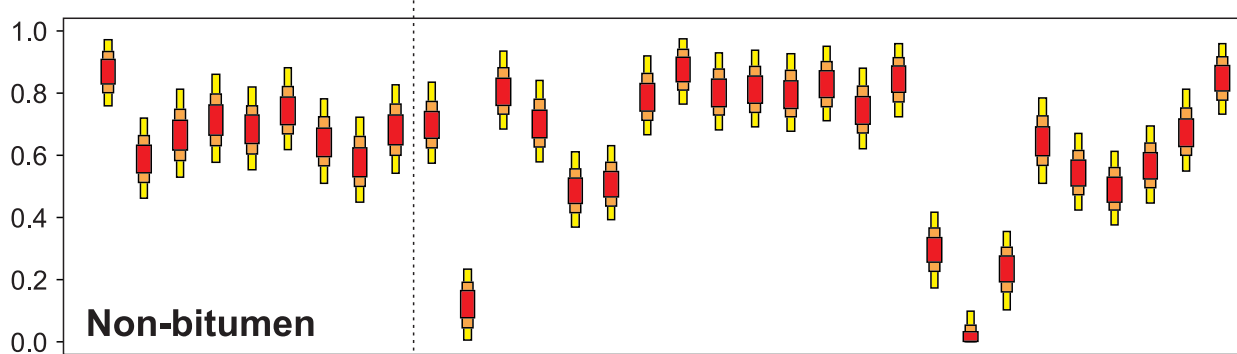
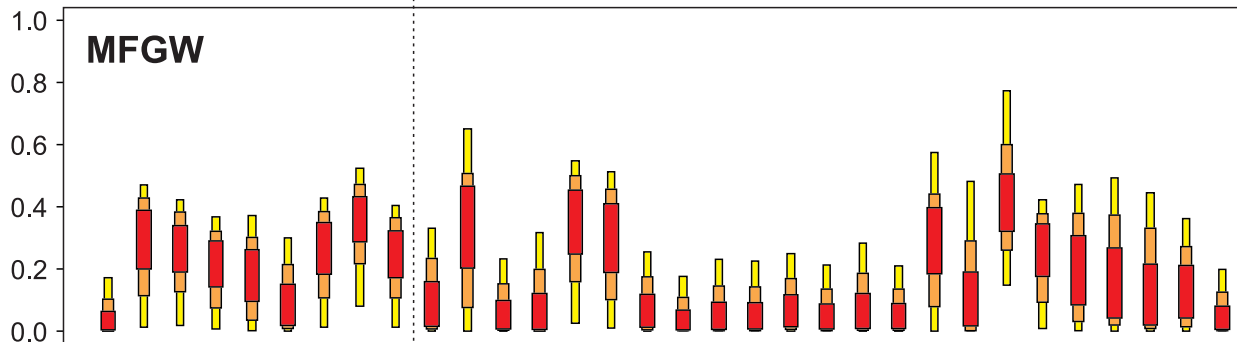
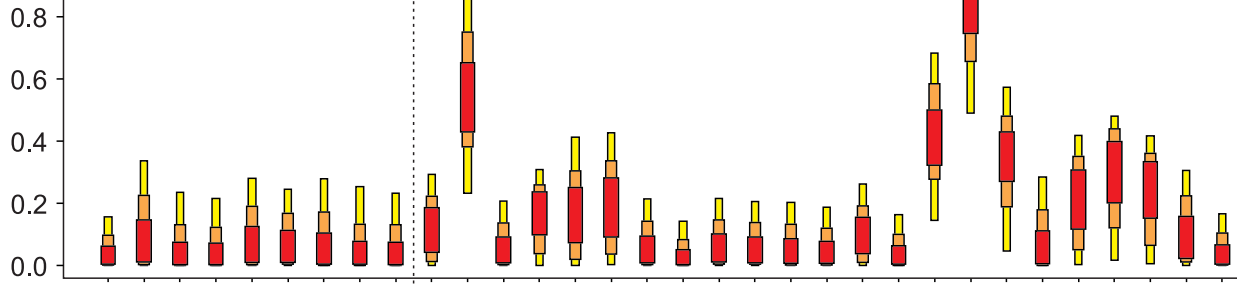


Proportion

**OSPW**

**MFGW**

**Non-bitumen**



GW1-1-2014  
 GW1-2-2014  
 GW1-3-2014  
 GW1-4-2014  
 GW1-5-2014  
 GW1-6-2014  
 GW1-7-2014  
 GW1-8-2014  
 GW1-9-2014  
 GW2-1-2015  
 GW2-2-2015  
 GW2-3-2015  
 GW2-4-2015  
 GW2-5-2015  
 GW2-6-2015  
 GW2-7-2015  
 GW2-8-2015  
 DP-25-2016  
 DP-17-2016  
 DP-24-2016  
 GW2-9-2016  
 DP-04-2016  
 GW2-3-2016  
 GW2-2-2016  
 DP-02-2017  
 DP-10-2017  
 DP-21-2017  
 DP-15-2017  
 DP-24-2017  
 GW2-7-2017  
 GW2-9-2017  
 GW2-3-2017

